Modeling Polymerization Reactions at Aluminum-Based Catalysts: Is DFT a Reliable Computational Tool?

Giovanni Talarico,[†] Vincenzo Barone,[†] Peter H. M. Budzelaar,[‡] and Carlo Adamo*[,§]

Dipartimento di Chimica, Università degli Studi di Napoli "Federico II", Complesso Monte S. Angelo, Via Cintia, I-80126 Napoli, Italy, Department of Inorganic Chemistry, University of Nijmegen, Toernooiveld 1, NL-6525 ED Nijmegen, The Netherlands, and Laboratoire d'Electrochimie et de Chimie Analytique, UMR 7575, ENSCP, 11 rue P. et M. Curie, F-75231 Paris Cedex 05, France

Received: April 10, 2001; In Final Form: June 14, 2001

A large number of DFT approaches, including classical GGA approximations, hybrid HF/DFT approaches, and more recent τ-dependent functionals, have been tested for olefin polymerization reactions at a cationic aluminum system, and their results have been compared with refined post-HF methods. The results show that hybrid density functional methods always outperform classical GGA approaches, and more recent τ-dependent functionals are not yet competitive, providing nonsystematic errors in the energy evaluations. The effect of the lengthening of the polymer chain from the "standard" ethyl group to a butyl group was found to be significant and hence has to be taken into account when predicting the molecular weight of polymers. A computational strategy to study olefin polymerization at Al systems is proposed.

1. Introduction

In the last 25 years, the polymerization of α-olefins promoted by single-site homogeneous catalysts has become a field of extraordinary interest from both experimental and theoretical points of view. In practice, every metal from the group 3 to the group 13 elements has been extensively investigated in olefin polymerization processes.[1,2] During the polymerization process, a complex equilibrium between different species associated with the precursor catalyst, the cocatalyst, the solvent, and the monomer, is present in solution.[3] In this context, quantum chemical computational methods have played a very useful role, elucidating the fascinating puzzle represented by the different steps involved in polymerization mechanisms.[4] However, due to the size of the system needed to reproduce a "realistic" chemical environment, standard post-Hartree−Fock (post-HF) calculations have so far been prohibitively expensive for most of the catalytic systems of practical interest. Luckily, the development of computational methods based on the density functional theory (DFT) is allowing the study of large systems without an unacceptable loss of accuracy.[5−7]

At the same time, the performance of different DFT models is strongly related to the functional form chosen for the exchange-correlation part.[5] This field is, therefore, in rapid evolution, and a number of functionals have been developed in the past few years (see, for instance, ref 7 for a review). As a matter of fact, the last generation of functionals, including, e.g., VSXC,[8] B98[9,] or HCTH[10] models, represents a significant improvement over more conventional approximations. Furthermore, we have found that hybrid HF/DFT models, such as B1LYP[11] or PBE0,[12] fix a number of problems, such as proton-transfer energy barriers or S_N2 thermochemistry.[12,13]

In this context, homogeneous catalysis is, in our opinion, an ideal playground to verify the reliability of new theoretical methods, since it couples a real chemical problem with several computational challenges, such as the size of the systems involved, the presence of significant electron correlation effects, and the transfer of light particles. In the particular case of α-olefin polymerization, the principal termination reactions involve the transfer of hydrogen atoms, which represent a "classic" DFT problem.[5]

SCHEME 1

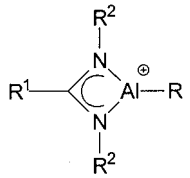

R^1 = H, R^2 = *iso*-propyl or

R^1 = *tert*-butyl, R^2 = *iso*-propyl

Following these lines, we report a detailed analysis on the ethylene reactions at aluminum−amidinate systems [{R^1C-(NR^2)$_2$}AlR] (see Scheme 1), which were recently reported to polymerize ethylene.[14,15]

The finding that these three-coordinated aluminum systems act as ethylene polymerization catalysts led to an explosion of interest in cationic aluminum alkyl compounds.[14] In our previous studies on the unsubstituted system with $R^1 = R^2 = H$ and R = C_2H_5, we found remarkable discrepancies between DFT (e.g., BP86 and B3LYP) and post-HF methods in the prediction of activation energies for the ethylene insertion and chain transfer steps involving the transfer of H atoms.[16,17] Furthermore, these discrepancies were different for the ethylene insertion and for the main chain termination steps: β-hydrogen transfer to the monomer (BHT), β-hydrogen transfer to the metal (BHE), and hydrogen transfer from the monomer to the alkyl chain by C−H activation (CHT). These findings could indicate that DFT methods are of limited use for the study of ethylene reactions promoted by this class of compounds.

* Corresponding author. E-mail: adamo@ext.jussieu.fr.
[†] Università degli Studi di Napoli "Federico II".
[‡] University of Nijmegen.
[§] ENSCP.

10.1021/jp011334t CCC: $20.00
Published on Web 09/06/2001

To rationalize these points, we have now tested a large number of DFT approaches and compared their results to each other and to post-HF data. The small size of the system with $R^1 = R^2 = H$ makes the latter task easier, allowing the use of sophisticated post-HF methods and of saturated basis sets.

Our goal is to find a trend for the differences or a systematic route to use DFT for olefin polymerization at aluminum systems, hoping that the errors can be corrected systematically or that new functionals can be developed. In addition, a study of the effects of several combinations of exchange and correlation functionals might provide additional insight into the DFT methods itself.

Since we have already shown that R^1 and R^2 substituents on the amidinate ligand do not play a crucial role in the ethylene reactions,[18] we have focused our attention on the representation of the growing polymer chain, which has been modeled either by an ethyl or by a butyl fragment. In fact, as far as we know, the effect of lengthening of the polymer chain in the computational modeling has only be checked in the context of γ-agostic interactions and BHE termination[19] and for the ethylene insertion at group 4 metallocene catalysts.[20] In the last part of the present paper, we propose an effective computational scheme for the study of Al systems, which incorporates corrections for known deficiencies in methods and model systems.

2. Computational Details

Both post-HF and DFT calculations were performed using a development version of the Gaussian package.[21]

A large set of exchange and correlation functionals was tested in the present study: some of them can be classified as "conventional" functionals and some others as "hybrid" functionals. The first class includes the BP and BLYP models, obtained by combining the Becke exchange with the Perdew or the Lee−Yang−Parr (LYP) correlation (a comprehensive list of conventional DFT approaches is given in ref 22). Next, the hybrid functionals known as B3LYP and B3PW91 have been tested, both use an empirical linear combination of Becke and HF exchange with the PW91 or the LYP correlation functional.[23] The B98 functional is the Becke 98 exchange-correlation functional in which just one parameter rules the HF/DFT exchange ratio.[9] We have also considered the so-called "parameter-free" model, in which the quantity of the HF exchange is fixed a priori to be 0.25.[12] In particular, the B1LYP variant is derived from BLYP,[11] while the mPW0 model is obtained using our modification of the PW exchange with the corresponding PW correlation[22,24] and the PBE0 model is generated from the exchange-correlation functional of Perdew, Burke, and Ernzerhof.[25] Finally, two different τ-functionals (i.e., functionals containing an explicit dependence upon the kinetic energy density) have been considered: the Scuseria's functional (VSXC)[16] and the B1Bc95 functional of Becke, in which the τ dependence is in the correlation part only.[8]

It must be pointed out that the PW exchange is derived from the B form, while the B98, PBE, and VSXC exchanges use a rational function of the reduced density. The difference between the different correlation forms is more drastic (see refs 5 and 7 for a discussion on this point), even if the PBE correlation is derived from the PW one.[25] All these functionals were already available in the Gaussian package or have been implemented by two of us, in a development version.[21]

Different Pople's basis sets have been considered.[22] Geometry optimizations have been carried out at the MP2 and B1LYP levels, using the 6-31G(d) basis sets, while single-point energy evaluations have been performed using the 6-311G(d,p) basis set. For the MP2 calculations, all electrons were included in excitation lists, and the results were compared with the frozen core approximation, leading to the conclusion that the frozen core increases the activation energies of 0.2−0.3 kcal/mol for all the reaction channels considered in the present study. We checked that the 6-31G(d) basis set is adequate for geometry optimizations comparing some structures with those obtained with 6-311G(d,p) basis set at the B1LYP level. Next, energy convergence was checked by adding step-by-step different sets of polarization and diffuse functions on all the atoms, up to the extended 6-311+G(3df, 2pd) level. This last basis set provides converged energies at both DFT and MP2 levels for several reactions, including proton transfer.[13,24] Please note that the basis set for Al referred to as 6-311G in the Gaussian package corresponds to the MacLean−Chandler basis set, contracted to a (631111/4211) pattern.[27]

All the stationary points located either at the MP2 or at the B1LYP levels have been characterized (as minima or first-order saddle points) by computing harmonic frequencies.

Single-point energy evaluations were performed also by the coupled cluster (CC) approach with single excitation, double excitation, and a perturbative estimate of triple excitation (CCSD(T)).[22]

Counterpoise corrections (CP) for the basis set superposition error (BSSE) were evaluated for olefin complexes according to the Boys−Bernardi method.[28]

3. Results

Two different molecular models have been used for the simulation of the growing polymer chain: in the small model, the chain is modeled as an ethyl moiety, while a butyl fragment is used in the large system. Several reaction paths have been considered for the small system (see Figure 1): starting from the bare aluminum-amidinate systems, $[\{HC(NH)_2\}Al\ C_2H_5]^+$ (R1), two reactive channels are possible, namely, the ethylene coordination with the formation of a π-complex (π-C2) and the β-hydride elimination (BHE), leading to the π-C8 complex. Next, three paths are open from π-C2: the ethylene insertion (TS3), the H-transfer from the monomer to the growing chain (CHT, structure TS6), and the β-H transfer to the monomer (BHT, TS5). The first two paths lead to the P4 and P6 products, respectively.

In Figure 2 are reported the corresponding reaction channels for the large model: analogous to R1, from the P4 product, two reactive channels are possible, the β-hydride elimination (BHE_{bu}, TS11, and P11) and the coordination of an ethylene monomer leading to the π-C12 complex. Next, two paths have been analyzed, one corresponding to the insertion mechanisms (TS13 and P14 structures) and the second to the BHT_{bu} reaction (TS15 and π-C16). This scheme allows us to verify the approximation in modeling the growing polymer chain on the two main termination steps reported for homogeneous catalysis of olefin polymerization.

The discussion of the results is divided into three main sections: the first part is devoted to the comparison of different computational models, with a particular attention to the performances of a representative collection of exchange-correlation functionals. In the second part, the chemical model is analyzed, and in particular, the effects of the lengthening of the polymer chain are discussed in detail. Finally, a combined DFT/MP2/CC approach is proposed and validated on the chosen systems.

3.1. Computational Model. *3.1.1. Geometries.* We have fully optimized all the molecular structures corresponding to the different steps of Figure 1, at both the MP2 and B1LYP levels.

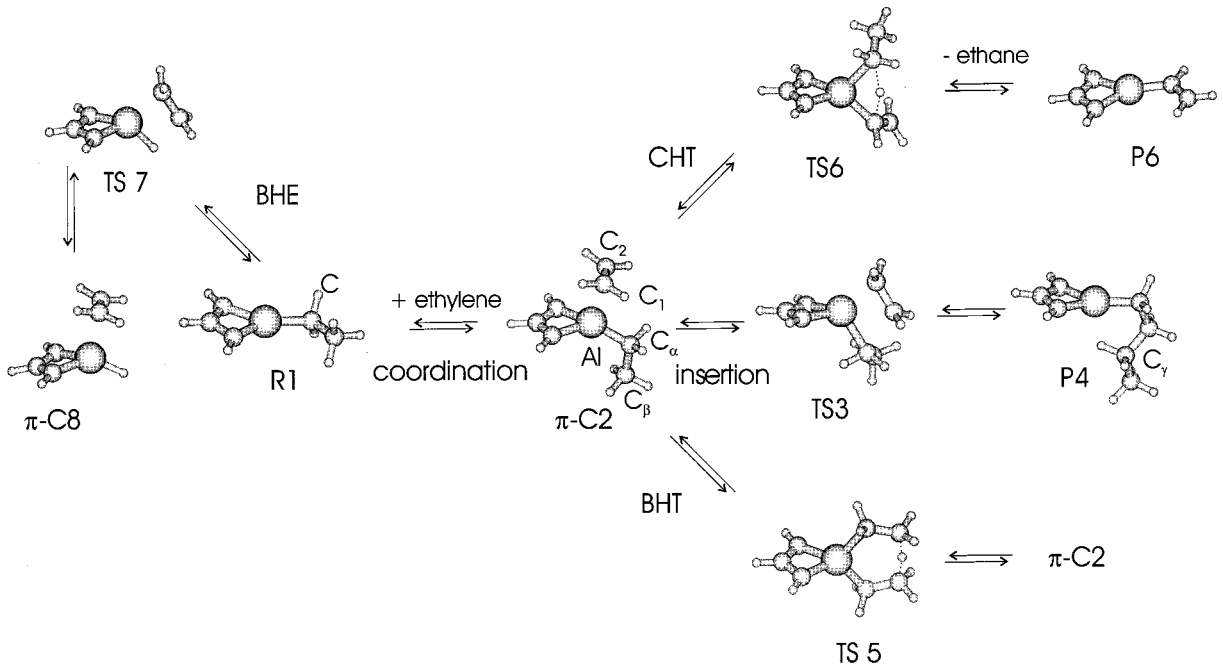

Figure 1. Schematic drawing and atom labeling for the molecular structures involved in the ethylene coordination, insertion, and transfer reactions. In the drawing, the growing chain is represented by an ethyl residue.

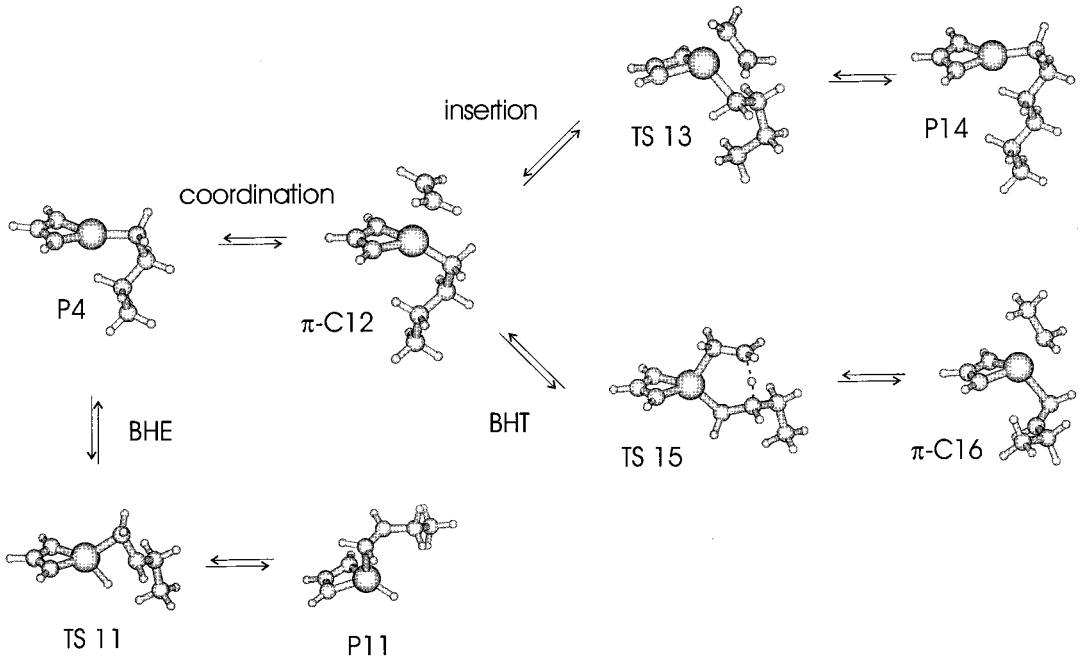

Figure 2. Schematic drawing and atom labeling for the molecular structures involved in the ethylene coordination, insertion, and transfer reactions. In the drawing, the growing chain is represented by a butyl residue.

It is well-known for organometallic systems that the B3LYP method provides better geometrical parameters than those of conventional functionals, like BP or BLYP (see for instance ref 5, 29, and 30). We have shown that the geometrical parameters provided by B1LYP, PBE0, and B3LYP are practically indistinguishable.[7] So, to avoid spurious effects in the successive energy comparisons, we prefer to consider only the geometries obtained by B1LYP computations. Anyway, we further assess the quality of these structures by some comparisons with MP2 results.

The geometrical parameters computed at the B1LYP and MP2 levels, reported in Table 1, are rather similar. Here we focus on the slight discrepancies found for the coordination complexes (π-C2 structure) and, in particular, for the ethylene−Al distance. In fact, the Al−C_2 length is 2.45 Å at the MP2 level, whereas B1LYP gives 2.52 Å.

Since these geometrical differences might play a relevant role in the assessment of the coordination step, and, hence, for the energetics of the whole reaction, we have investigated this point by a comparison of single-point CCSD(T) energies obtained with MP2 and B1LYP structures.

The results collected in Table 2 clearly show that the two data sets are close to each other, the difference being never larger than 0.2 kcal/mol. These results point out how the discrepancies found in the geometry of the π-complexes do not affect energetic parameters, due to the flatness of the potential energy surface

TABLE 1: Selected Geometrical Parameters (Å and Degrees) Calculated at the MP2 and B1LYP Levels for the Structures Reported in Figure 1, Using the 6-31G(d) Basis Set[a]

geometrical parameters	MP2	B1LYP	MP2	B1LYP
	R1		TS7	
$C_\alpha-C_\beta$	1.541	1.546	1.422	1.431
$Al-C_\alpha$	1.929	1.937	2.020	2.023
$Al-H_\beta$	3.145	3.183	1.655	1.661
$Al-C_\alpha-C_\beta$	114.1	115.4	62.5	79.8
	π-C8		P6	
$C_\alpha-C_\beta$	1.357	1.352	1.353	1.347
$Al-C_\alpha$	2.432	2.468	1.897	1.897
$Al-H_\beta$	1.560	1.559	2.958	3.019
$Al-C_\alpha-C_\beta$	79.0	74.2	118.6	121.3
	π-C2		TS 3	
$Al-C_1$	2.452	2.519	1.984	1.975
$Al-C_2$	2.452	2.515	2.205	2.247
C_1-C_2	1.352	1.350	1.439	1.453
$Al-C_\alpha$	1.935	1.943	2.062	2.095
$C_\alpha-C_\beta$	1.541	1.546	1.530	1.534
$C_\alpha-C_2$	3.561	3.614	2.213	2.210
$Al-C_\alpha-C_\beta$	112.3	113.9	78.4	80.3
$Al-C_1-C_2$	74.0	74.3	78.4	80.3
	TS 5		TS6	
$Al-C_1$	2.037	2.042	2.015	2.013
$Al-C_\alpha$	2.037	2.042	2.055	2.078
C_1-C_2	1.443	1.452	1.356	1.356
$C_\alpha-C_\beta$	1.443	1.452	1.541	1.543
C_2-H	1.291	1.312	2.200	2.258
$C_\beta-H$	1.291	1.312	2.652	2.607
Al−H	2.803	2.816	1.675	1.687
$C_\beta-C_2$	2.568	2.600	4.057	4.125
C_1-Al-C_α	103.4	104.3	92.1	92.6
C_2-H-C_β	168.3	167.4	112.5	115.8
	P4			
$Al-C_\alpha$	1.929	1.940		
$C_\alpha-C_\beta$	1.543	1.549		
$C_\beta-C_\gamma$	1.529	1.536		
$C_\gamma-H_\gamma$	1.124	1.129		
$Al-H_\gamma$	2.127	2.218		
$Al-C_\alpha-C_\beta$	101.2	104.4		
$C_\alpha-C_\beta-C_\gamma$	110.5	111.2		
$Al-C_\alpha-C_\beta-C_\gamma$	324.5	323.5		

[a] Atom numbering scheme: $H_2C^1{=}CH_2^2$ for the olefin and $Al-C_\alpha-C_\beta-C_\gamma$ for the growing chain.

TABLE 2: Total CCSD(T) Energies (Hartrees) and Energy Differences (kcal/mol) Computed Using the 6-31G(d) Basis Set and the MP2 or B1LYP Geometries

	B1LYP geometry	MP2 geometry	ΔE^a
π-C8	−469.71006267	−469.71000867	−0.03
TS7	−469.67042619	−469.67026373	−0.10
R1	−469.72974229	−469.72968171	−0.04
π-C2	−548.08752902	−548.08756822	0.02
TS3	−548.03785059	−548.03741168	−0.28
P4	−548.09968376	548.09954261	−0.09
TS5	−548.04736900	−548.04701675	−0.22
TS6	−547.99893147	−547.99913447	0.13
P6	−468.52430639	−468.5244676	0.10

[a] CCSD(T)/B1LYP-CCSD(T)/MP2.

(PES) governing ethylene coordination. Similar results (within 0.1 kcal/mol) were obtained by CCSD(T) energy evaluations at B1LYP/6-311G(d,p) geometries.

Even if both geometry sets give close CC energies, post-HF energy evaluations have been carried out employing MP2 structures, while B1LYP geometries will be used in the following for all the DFT computations.

3.1.2. Energetics. As mentioned above, CC computations give reliable energy results, provided that a saturated basis set is used. This is, of course, not an easy task, due to the great resource demand of the method. As a matter of fact, mixed methods that combine low-level geometries with CC single-point energy evaluations and basis set extrapolations like the Gn family (i.e., G1, G2,[31,32] and, more recently, G3[33]) reach the so-called "chemical accuracy" for molecular energies. Of course, the consistency of the method rests on the soundness of the extrapolations used and, in particular, on the availability of basis-set converged results.

In the same spirit, we thought that reliable results can be obtained by combining CCSD(T)/6-31G(d) energies with basis set extension effects computed at the MP2 level. To find the smallest basis set providing converged results, we have analyzed the basis set dependence of the MP2 results for all the reactive steps of the small model. In particular, we have considered a large set of basis sets, ranging from 6-31G(d) to 6-311+G(3df,-2pd). The results, reported in Table 3, have been next compared with the G3large basis,[34] that is, 6-311+G(2df,2p) on first-row atoms and 6-311+G(3d2f) on Al.

We note that for all the cases considered, convergence is reached at the 6-311+G(2df,2pd) level. This basis set is slightly larger than that used in the G3 approach. In particular, we have found that all the steps involving a hydrogen transfer are sensitive to a supplementary *d* function on hydrogen atom, while the effect of the third *d* as polarization function on Al is always negligible.

Our best estimates for the whole reaction energetics were next obtained by adding to the CCSD(T)/6-31G(d) values the MP2 basis set extrapolation, that is, the difference between MP2/6-311+G(2df,2pd) and MP2/6-31G(d) results. These values are reported in the last column of Table 4 and will be our reference values ("best value"). It is worth noting that we tested the validity of basis set extrapolation at the MP2 level by comparing actual CCSD(T)/6-311G(d,p) values with extrapolated results obtained adding to CCSD(T)/6-31G(d) values the difference between the MP2/6-311G(d,p) and the MP2/6-31G(d) results. The differences are never larger than 0.3 kcal/mol.

In Table 4 are reported the reaction and activation energies for all the steps of Figure 1. Among the functionals considered, we have reported in the table only the results obtained with the BP86, the B1LYP, and the VSXC approaches. These functionals have been chosen as the most representative of the family of conventional (BP86), hybrid (B1LYP), and τ-dependent (VSXC) functionals. To cover the full range of the basis sets considered, we have collected in the table the results obtained with the smallest (6-31G(d)) and the largest (6-311+G(2df,2pd)) ones. A complete list of energies, referring to all the considered functionals, is available as Supporting Information (table S-I).

Let us start from the BHE, which is the reaction leading from R1 to π-C8, through TS7. The reaction energies (ΔE_{BHE}) do not show a strong dependence on the functional, and the values (12−16 kcal/mol) agree well with the CCSD(T) value of 13.8 kcal/mol. The only exception is the VSXC functional, which predict an endothermicity of only 8.1 kcal/mol.

A clear trend is present, instead, for the corresponding activation energies ($\Delta E^{\#}_{BHE}$). Here, the conventional functionals (BP86 and BLYP) give almost the same barrier (about 32 kcal/mol), with the BP86 result marginally lower than the BLYP one. The inclusion of some HF exchange increases the barrier height, irrespective of the specific form of the exchange and correlation functionals. The B1LYP value is slightly higher than the others, and it is the closest to the post HF results (about 35

TABLE 3: Basis Set Influence at the MP2 Level on the Energies of Different Reactions Relative to the π-Complex π-C2[a]

method	N° basis function	$\Delta E^{\#}_{BHE}$[b]	ΔE_{BHE}[b]	ΔE_{coor}	$\Delta E^{\#}_{ins}$	ΔE_{ins}	$\Delta E^{\#}_{BHT}$	$\Delta E^{\#}_{CHT}$	ΔE_{CHT}
6-31G (d)	148	39.2	14.0	24.0	30.6	−9.3	24.7	54.1	18.8
6-31G (d,p)	184	39.8	15.3	23.8	30.2	−10.0	23.0	52.0	18.7
6-31+G(d)	180	38.9	13.5	23.2	31.3	−8.7	24.9	54.0	19.2
6-31+G(d,p)	216	39.2	14.8	22.8	31.0	−9.0	23.1	52.0	18.9
6-311G (d,p)	224	38.7	16.1	22.6	28.9	−10.9	21.4	49.1	18.3
6-311G (2d,p)	264	38.7	15.8	23.1	28.5	−9.8	21.2	48.3	18.7
6-311+G (2d,2p)	332	38.3	15.6	23.9	28.4	−9.6	20.9	48.2	18.9
6-311+G (2df,2pd)	448	37.4	15.4	23.3	27.5	−10.2	20.6	47.2	19.7
mixed basis set[c]	344	38.5	15.9	22.6	28.4	−10.6	20.8	47.9	19.1
G3large[d]	400	37.4	15.9	23.2	27.5	−9.7	21.1	47.6	19.6

[a] All the values are in kcal/mol and are not corrected for BSSE. [b] Relative to R1. [c] 6-31+G(d) on Al and on the amidinate ligand ($HC(NH)_2$), 6-311+G (2df,2pd) on the olefin and the growing chain. [d] G3large-like basis set.

TABLE 4: Calculated Energies (kcal/mol) for Reactions of Al−Et Species (π-C2): β-H Transfer to the Metal ($\Delta E^{\#}_{BHE}$ and ΔE_{BHE}), Ethylene Coordination (ΔE_{coor}), Insertion ($\Delta E^{\#}_{ins}$ and ΔE_{ins}), β-H Transfer to the Monomer ($\Delta E^{\#}_{BHT}$), and H Transfer to the Chain ($\Delta E^{\#}_{CHT}$ and ΔE_{CHT})

basis set: A = 6-31G(d) B = 6-311+G(2df,2pd)	BP86[a]		B1LYP[a]		VSXC[a]		MP2[b]		CCSD(T)[b]	
	A	B	A	B	A	B	A	B	A	best value [c]
$\Delta E^{\#}_{BHE}$[d]	31.7	30.7	35.4	34.0	26.8	26.5	39.4	37.4	37.3	35.3
ΔE_{BHE}[d]	15.9	16.5	14.8	15.0	8.1	7.9	14.0	15.4	12.4	13.8
ΔE_{coor}[e]	15.9	17.5	17.4	15.7	25.6	25.8	18.9	21.4	17.6	20.1
	(2.9)	(0.5)	(2.6)	(0.5)	(3.2)	(0.8)	(5.1)	(1.8)	(5.0)	(1.7)
$\Delta E^{\#}_{ins}$	22.5	22.1	28.6	28.3	21.0	21.8	30.6	27.3	31.5	28.2
ΔE_{ins}	−9.7	−9.0	−8.0	−6.9	−4.4	−2.9	−9.0	−10.2	−7.5	−8.7
$\Delta E^{\#}_{BHT}$	9.7	9.3	17.9	17.7	15.4	16.3	25.0	20.6	25.4	21.0
$\Delta E^{\#}_{CHT}$	43.5	40.3	50.6	47.1	46.4	44.3	54.2	47.5	55.5	48.8
ΔE_{CHT}	16.9	19.4	14.7	12.8	23.5	23.4	18.8	19.7	18.1	19.0

[a] Computed using B1LYP/6-31G(d) geometries. [b] Computed using MP2/6-31G(d) geometries. [c] Best value = ΔE(CCSD(T)/6-31G(d)) + ΔE(MP2/6-31G(d)) − ΔE(MP2/6-311+G(2df,2pd)). [d] Relative to reactant 1 (R1). [e] The values are corrected for the BSSE; correction given in parentheses.

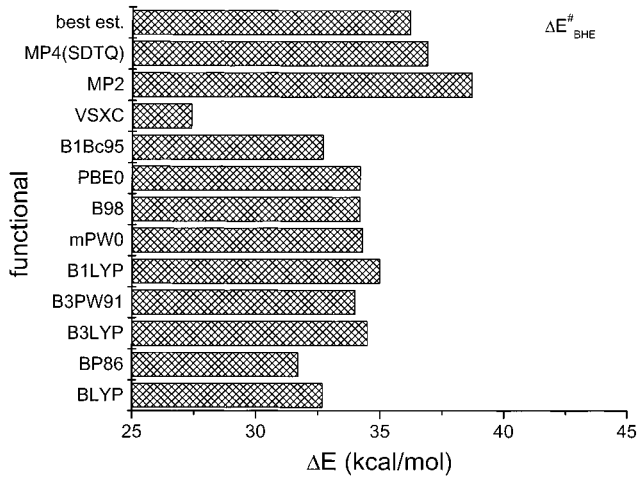

Figure 3. Histogram representation of the activation energy for the β-hydrogen elimination (BHE) reaction. All the DFT and MP2 values have been computed with the 6-311G(d,p) basis set.

kcal/mol). The histogram representation of Figure 3, collecting the results obtained with the 6-311G(d,p) basis set, underlines this trend and illustrates two further points. First, it is interesting to note that the MP2/6-311G(d,p) computational model overestimates the barrier (+3.1 kcal/mol). The inclusion of higher excitations (MP4(SDTQ)) leads to a lower value, even if still higher than the CC estimation (35.3 kcal/mol). Concerning τ-functionals, the B1Bc95 model has a behavior intermediate between pure and hybrid functionals, probably due to the inclusion of some HF exchange, while the prediction of the VSXC variant is very low (26.5 kcal/mol), possibly as a consequence of the less endothermic reaction energy.

The coordination of an ethylene monomer to R1 leads to the π-C2 complex (ΔE_{coor}). The striking feature of the data reported in Table 4 is the VSXC result for the coordination energy (25.8 kcal/mol), which is about 6 kcal/mol higher than the reference CC value (20.1 kcal/mol). As concerns the other functionals, a slight effect of the exchange and correlation can be inferred from the collected data. In particular, functionals including the LYP correlation underestimate the coordination energy, and even inclusion of some HF exchange does not cause a significant improvement (16.0 and 18.0 kcal/mol for the BLYP and the B3LYP methods, respectively). A better agreement is found if the PW correlation or more recent functionals are considered. So, for instance, the mPW0 functional gives 21.2 kcal/mol, while the PBE0 result is slightly higher (22.2 kcal/mol; see table S-I).

Next, we can examine the three reactive channels, which lead from π-C2 to TS3, TS5, and TS6. As explained above, these last three channels correspond to the chain propagation (TS3) and to two termination reactions (TS5 and TS6). Let us begin the discussion with propagation, whose representative energies are reported in Table 4. In Figure 4 are reported the activation energies for TS3 obtained with different methods and the 6-311G(d,p) basis set.

The results for both activation and reaction energies are spread over a wide range, without any systematic dependence on the nature of the functional (conventional, hybrid or τ-dependent). For the reaction energy (ΔE_{ins}), the VSXC provides the worste values (−4.1 kcal/mol,), compared to the best estimation (−8.7 kcal/mol).

In a similar manner, the activation energies ($\Delta E^{\#}_{ins}$) range from 22 kcal/mol at the BP86 and VSXC levels to 28 kcal/mol obtained with the B1LYP functional. This last value matches the CC results. The role of the correlation functional in

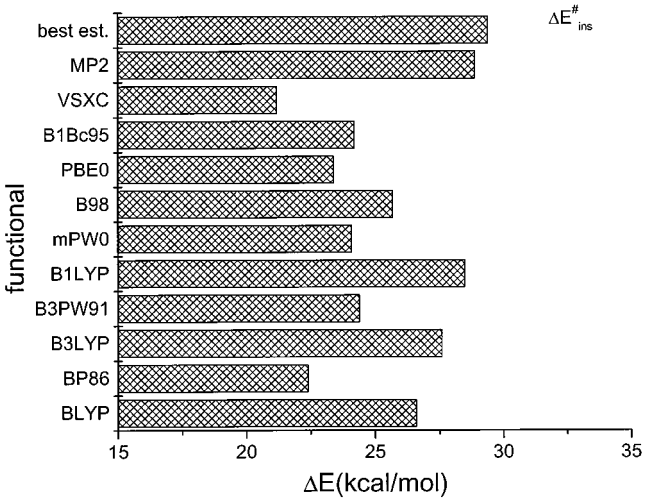

Figure 4. Histogram representation of the activation energy for the insertion step. All the DFT and MP2 values have been computed with the 6-311G(d,p) basis set.

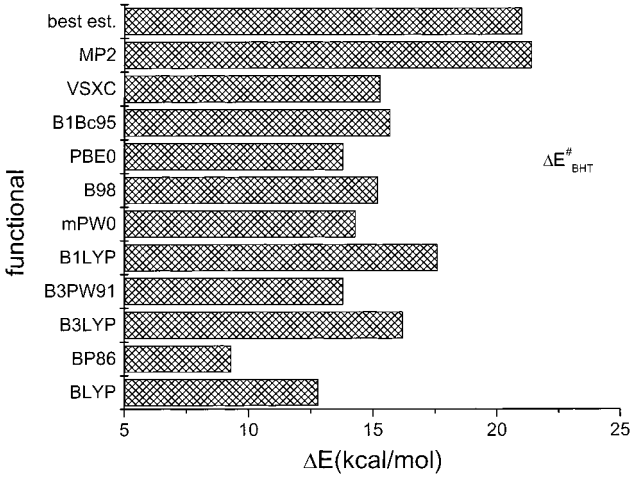

Figure 5. Histogram representation of the activation energy for the β-hydrogen transfer to the monomer (BHT) reaction. All the DFT and MP2 values have been computed with the 6-311G(d,p) basis set.

determining the barrier height is evident from a comparison of BP86 and BLYP results (22.4 and 26.6 kcal/mol, respectively; see Table 4). At the same time, the B3LYP estimate is about 3 kcal/mol higher than the B3PW91 one (27.6 vs 24.4 kcal/mol, respectively). In this last case, the increase of HF exchange contribution has a relatively small effect on the computed energy, BLYP, B3LYP, and B1LYP values being 26.6, 27.6, and 28.5 kcal/mol, respectively.

The second termination reaction corresponds to the CHT channel (TS6). Here all the conventional DFT methods underestimate the barrier height, with respect to the CC reference value (48.8 kcal/mol). Hybrid methods provide a significant improvement so that the B1LYP value (47.8 kcal/mol) is the very close to the CC estimate. It must be noted that except for the BP result, all the methods give results within a small interval around 44 kcal/mol (see also Figure S1).

A different behavior is found for the thermodynamics of the reaction (ΔE_{CHT}, see Table 4). Here, as it found for the coordination step, the VSXC functional provides the highest value (23.4 kcal/mol), about 4 kcal/mol higher than the best estimation (19.0 kcal/mol). Next, B1LYP slightly stabilizes the products ($\leq$ 13 kcal/mol), while the BP86 result is in good agreement (19.4 kcal/mol; see Table 4).

The β-hydrogen transfer from the growing chain to the monomer represents the last termination channel. In the small model, this step involves a symmetric transition-state structure (TS5), which joins two equivalent metal−olefin complexes (π-C2). All the DFT methods provide barriers ($\Delta E^{\#}_{BHT}$; see Figure 5) lower than the reference CC value of 21.0 kcal/mol. In this context, the B1LYP model, thanks to the relevant HF contribution, partially corrects the faults of the parent BLYP and B3LYP functionals, its value being about 3 kcal/mol lower than the MP2 and CC estimations.

The BP86 functional gives the lowest value (<10 kcal/mol), while all the other functionals provide results ranging between 14 kcal/mol (B3PW91) and 15 kcal/mol (VSXC). It must be noticed that BHT is the only channel for which none of the DFT methods used is able to produce an accurate result. B1LYP, which for the other reactions matches the CC extrapolated results within 1 kcal/mol, can only partially correct this fault.

Some trends can be inferred from our results. In particular, the BHE and the insertion reactions present some common aspects. In fact, the results show a similar pattern, with the VSXC functional strongly underestimating the insertion and the P86 correlation functional performing better than its LYP counterpart. At the same time, HF exchange plays a minor role in determining the absolute energy values.

All the termination processes (BHE, CHT, and BHT) correspond to hydrogen transfer (HT) reactions. Actually, it is well-known that activation energies for proton and hydrogen transfer are significantly underestimated by DFT methods.[35,36] Hybrid approaches, such as B1LYP, can partially solve this problem, providing results significantly closer to those obtained by post HF methods.[35] The activation energies computed for the three reactions confirm this trend, all the DFT results being (to different extents) lower than the reference CC computations. These differences between post-HF and DFT results depend on the nature of the hydrogen being transferred. So a strong dependence upon both the exchange and the correlation functional is found for the CHT and BHE steps, where the short metal−hydrogen distance suggests HT assisted by the heavy atom. Here the LYP correlation performs better than its P86 and PW counterparts, and the inclusion of some HF exchange significantly improves the final results (B1LYP > B3LYP > BLYP). For the BHT, which can be considered a "true" HT, all the hybrid methods provide similar results, while the conventional BLYP and BP functionals give results close to each other. In short, all the considered DFT approaches regardless of their origin give barriers that are too low, the B1LYP model being the most accurate in the three cases. Finally, the poor performances of the VSXC functional in describing the CHT, insertion, and the BHT paths can be rationalized in terms of excessive stabilization of π-complexes.

As a last point concerning the small systems, we have checked the effect of the basis set on the computed DFT energies. To this end, we compared the 6-31G(d) and 6-311+G(2df,2pd) results of Table 4. All DFT computations are only marginally affected by the basis set extension, and converged results, within 0.7 kcal/mol, have been obtained with the 6-311G(d,p) basis set. This is in striking contrast with the MP2 computations discussed in a previous section (see Table 3).

In summary, our computations suggest that the choice of the correlation functional is crucial for an accurate description of the insertion step, the LYP functional providing the most accurate results. In all the cases where the transfer of a proton is the key step, inclusion of some HF exchange is essential to correct the problems shown by exchange functionals. Furthermore, our results stress that conventional density functionals

TABLE 5: Selected Geometrical Parameters (Å and deg) Calculated at the MP2 and B1LYP Levels for the Structures Reported in Figure 2, Using the 6-31G(d) Basis Set[a]

geometrical parameters	MP2	B1LYP	MP2	B1LYP
	π-C12		π-C16	
Al−C_1	2.449	2.508	2.317	2.285
Al−C_2	2.471	2.549	2.894	2.935
C_1−C_2	1.353	1.350	1.540	1.545
Al−C_α	1.937	1.946	1.938	1.950
Al−C_α−C_β	112.5	115.2	82.3	92.8
	TS 13		P14	
Al−C_α	2.044	2.086	2.774	2.788
Al−C_1	1.992	1.997	1.940	1.940
Al−C_2	2.203	2.247	2.742	2.749
C_1−C_2	1.435	1.453	1.550	1.550
C_α−C_β	1.532	1.539	1.532	1.533
C_α−C_2	2.233	2.212	1.536	1.536
Al−C_1−C_2	78.2	80.3	103.0	103.4
C_1−Al−C_α	102.2	100.5	62.4	62.0
	P11		TS11	
Al−C_α	2.294	2.253	1.995	1.991
C_α−C_β	1.361	1.365	1.438	1.455
C_β−C_γ	1.495	1.491	1.494	1.498
C_γ−H_γ	3.539	3.768	1.095	1.096
Al−H_γ	1.562	1.562	3.292	3.373
Al−C_α−C_β	81.8	92.7	81.2	82.6
C_α−C_β−C_γ	125.3	126.2	123.0	123.4
Al−C_α−C_β−C_γ	−90.8	−91.4	108.2	109.6
	TS 15			
Al−C_1	2.079	2.084		
Al−C_α	1.997	2.002		
C_1−C_2	1.415	1.423		
C_α−C_β	1.477	1.490		
C_2−H	1.402	1.456		
C_β−H	1.215	1.221		
Al−H	2.774	2.798		
C_β−C_2	2.604	2.662		
C_1−Al−C_α	104.3	105.5		
C_2−H−C_β	168.6	167.8		

[a] Atom numbering scheme: $H_2C^1{=}CH_2^2$ for the olefin and Al−C_α−C_β−C_γ for the growing chain.

(here BP86 and BLYP) are not reliable enough for studying olefin reactions involving aluminum species. Similar results have been already obtained for selected functionals for a number of Al complexes.[37−39] Among all the functionals, the B1LYP variant provides "on average" the best performance.

3.2. Chemical Model. As mentioned in the Introduction, DFT computations have become invaluable tools in the study of the mechanism of ethylene polymerization at different catalytic sites.[4] Unfortunately, the large size of the systems under investigations dictates the use of simplified models of the active centers (see for instance refs 40−42). In particular, the growing polymer chain is commonly modeled by an ethyl unit, the smallest system capable of β-agostic interaction.[40−42] The relatively small size of our systems allows the removal of this constraint and a further investigation of this point. Specifically, we have considered insertion and transfer reactions involving a butyl chain as model chain. For the transfer reactions, we focused our attention on the intramolecular reaction involving the β-transfer to the metal (BHE_{bu}) and the intermolecular reaction involving the β-H transfer to the monomer (BHT_{bu}), which are the main chain transfer reactions occurring with homogeneous catalysts (depending on the experimental conditions like monomer concentration and reaction temperature). The fully optimized geometrical parameters of the structures sketched in Figure 2 are reported in Table 1 for P4 and in Table 5 for the other stationary points.

These results clearly show that the nature of the growing chain has only a slight effect on the molecular rearrangements. So all the trends observed for the small systems are preserved in the large model, including the differences between post-HF and B1LYP results. Small differences are found for only few geometrical parameters, like Al−C_α in TS3 and in the corresponding TS13 or the agostic Al−H_γ interaction in the products P4 and P14. More significant variations are observed for the BHT transition states (TS5 and TS15). First of all, we remark that the ethyl-to-ethylene transition state (TS5) is symmetrical, with the transferred H atom equidistant from two-ethylene moieties, whereas this is not the case for the transfer to a butyl chain. As a consequence, after the H-transfer, a new product (P16) is obtained, in which a 1-butene is coordinated to an amidinate Al−ethyl chain (see Figure 2). This reaction has an earlier transition state, with a larger C_β−C_2 distance and the moving hydrogen atom closer to C_β than to C_2. Accordingly, a decrease of all the activation energies is observed when extending the growing chain (see Table 6).

Both DFT and post-HF methods predict an olefin coordination energy which is about 2 kcal/mol lower than that for the ethyl chain. For instance, the coordination energy is 15.2 kcal/mol at the B1LYP level (−2.2 kcal/mol with respect to ethyl) and 16.0 kcal/mol at the CCSD(T) level (−1.6 kcal/mol). Smaller variations (<1 kcal/mol) are found for the insertion step. As a consequence, the CCSD(T) estimate for the coordination and insertion steps obtained for the large system (and including the effect of the basis set extension) are close to the values obtained at the B1LYP level with the small basis set. In particular, the coordination energy is 17.4 kcal/mol at the B1LYP/6-31G(d) level for the ethyl system (see Table 4), while the best value for the butyl model is 17.3 kcal/mol (see Table 6). In a similar manner, the activation energy and the exothermicity for insertion are 28.6 and −8.0 kcal/mol at the B1LYP level for the small complex and 28.9 and −7.5 kcal/mol for the large complex at the CC level.

A larger variation is found, instead, for the BHE_{bu} and BHT_{bu} steps. In the former case, using a butyl chain in place of an ethyl chain decreases the activation energy by 3−6 kcal/mol for all computational methods (see Figure S2); in the latter case, this decrease is between 3 and 4 kcal/mol.

The effects of the lengthening of the polymeric chain on the termination steps together with the marginal effect reported on the propagation step are definitely not negligible. This means that one should be careful in the selection of computational tools able to predict a correct balance between propagation and termination steps. We recall that this balance is responsible for the molecular weight of the resulting polymers, which is one of the most important experimental parameters.

All the other trends found for the ethyl chain (e.g., the effect of the basis set or the difference between functionals) are preserved upon lengthening of the growing chain.

The agreement between the final B1LYP result for the BHT on the small system and the small basis set (17.7 kcal/mol) and the best value obtained by CCSD(T) for the large system (18.2 kcal/mol) is only due to an accidental compensation of the various effects. Nevertheless, this accidental compensation can be useful as a cheap way to estimate the balance between insertion and termination steps for new Al-systems.

3.3. Effective Computational Model. The results discussed in the previous sections show on one hand that that B1LYP geometries are at least as good as MP2 ones (but these latter sometimes exhibit a very slow convergence[43]) and on the other hand that MP2 basis set extension provides reliable energy

TABLE 6: Calculated Energies (kcal/mol) for Reaction of the Al−Bu Species (π-C12): β-H Transfer to the Metal ($\Delta E^{\#}_{\mathrm{BHEbu}}$ and $\Delta E_{\mathrm{BHEbu}}$), Ethylene Coordination (ΔE_{coor}), Insertion ($\Delta E^{\#}_{\mathrm{INSbu}}$ and $\Delta E_{\mathrm{INSbu}}$), and β-H Transfer to the Monomer ($\Delta E^{\#}_{\mathrm{BHTbu}}$ and $\Delta E_{\mathrm{BHTbu}}$)

basis set: A = 6-31G(d) B = 6-311+G(2df,2pd)	BP86[a]		B1LYP[a]		VSXC[a]		MP2[b]		CCSD(T)[b]	
	A	B	A	B	A	B	A	B	A	best value [c]
$\Delta E^{\#}_{\mathrm{BHEbu}}$[d]	26.4	25.8	28.7	26.7	23.1	24.3	34.0	33.3	31.7	31.0
$\Delta E_{\mathrm{BHEbu}}$[d]	10.3	11.0	8.6	8.9	3.6	4.0	9.5	11.8	8.1	10.4
ΔE_{coor}[e]	15.6	14.0	15.2	13.5	26.0	23.7	17.1	18.4	16.0	17.3
	(2.3)	(0.4)	(2.6)	(0.4)	(2.9)	(0.9)	(4.8)	(1.8)	(4.7)	(1.7)
$\Delta E^{\#}_{\mathrm{INSbu}}$	22.9	22.6	28.9	28.7	23.2	23.9	30.8	28.1	32.1	28.9
$\Delta E_{\mathrm{INSbu}}$	−9.5	−8.8	−7.9	−6.9	−0.7	−1.2	−8.1	−9.0	−6.6	−7.5
$\Delta E^{\#}_{\mathrm{BHTbu}}$	6.7	6.4	14.2	14.1	14.3	15.8	20.5	17.0	21.7	17.9
$\Delta E_{\mathrm{BHTbu}}$[e]	−8.1	−7.7	−7.5	−7.3	−8.0	−8.1	−5.5	−5.7	−5.2	−5.4
	(2.5)	(0.6)	(2.3)	(0.5)	(2.6)	(0.7)	(2.5)	(0.9)	(0.8)	(−0.9)

[a] Computed using B1LYP/6-31G(d) geometries. [b] Computed using MP2/6-31G(d) geometries. [c] Best value = ΔE(CCSD(T)/6-31G(d)) + ΔE(MP2/6-31G(d)) − ΔE(MP2/6-311+G(2df,2pd)). [d] Relative to product 4 (P4). [e] The values are corrected for the BSSE; correction given in parentheses.

corrections to CC computations. So we have thought it useful to investigate a "composite model", analogous to the G2-(B3LYP/MP2/CC) method proposed by Bauschlicher and Partridge[43] or to the more recent G3(B3LYP) variant,[43] for combining DFT and post-HF results. The efficacy of such a method rests on the more or less favored balance between "numerical performance" and computer requirement. The largest basis set considered here (6-311+G(2df,2pd)) is quite large, and some reduction is in order for larger systems. One possibility is to use different basis sets for different atomic centers. Some hints on this point come from an analysis of the MP2 energy results of Table 3. In fact, these data show a first gap of about 2 kcal/mol in going from the 6-31G(d,p) to the 6-311G(d,p) basis set and a second gap, of about 1 kcal/mol, upon the inclusion of f polarization functions on heavy atoms and of d functions on hydrogens (from 6-311+G(2d,2p) to 6-311+G-(2df,2pd)). To verify the origin of these effects, we have carried out some MP2 computations using mixed basis sets on the two structures relevant for the activation energy of the BHT (see Table S-II of Supporting Information). In particular, the computations carried out with the 6-31G(d,p) basis set for the Al and the 6-311G(d,p) for all the other atoms are practically identical to those obtained with the 6-311G(d,p) on all the atoms. This shows that the 6631/631 basis set of Pople[45] already provides an accurate description of the Al atom, while this is not the case for the organic moiety, which requires at least a triple-ξ description. A similar behavior is found for the CHT reaction. At the same time, the amidinate ligand can be treated at a lower level, since the 6-31G+(d) basis set already provides converged results.

In short, nearly converged results are obtained using the 631+G(d) basis set for Al and the amidinate ligand and the 6-311+G(2df,2pd) basis on the growing chain, as well as on the incoming monomer. The resulting basis set (labeled "mix" in Table 3, 344 functions) is significantly smaller than both the G3 large (400 functions) and the 6-311+G(2df,pd) (448 functions) basis sets. A further reduction of the basis set should be possible if long-range interactions are not present between the catalytic center and the growing chain (e.g., γ-agostic interactions). In this case, the atoms belonging to the more distant chain units can also be represented by the small 6-31+G-(d) basis set. Since our systems are rather small, we have not checked this hypothesis.

Combining all the above results, a viable way to obtain reliable energy estimates at a relatively low cost can be envisaged. It is represented by a multilayer approach in which different post-HF and DFT methods are employed:

(a) DFT geometry optimizations and evaluations of ZPE corrections by hybrid HF/DFT models, (e.g., B1LYP, B3LYP, or PBE0) with 6-31G(d) or, when possible, 6-31+G(d) basis sets. Note that the ZPE corrections correction is small anyway and its evaluation at the HF or MP2 level would also be acceptable (see refs 16 and18). Nevertheless, the correction is necessary for prediction of the molecular weight since it is different for insertion reaction and BHT (see refs 16 and 18).

(b) CC energies obtained on the small system (growing chain = ethyl) with the 6-31G(d) basis set.

(c) Extrapolation to large basis set at the MP2 level. We tested the validity of this extrapolation by comparing CCSD(T)/6-311G(d,p) values with the extrapolated results obtained adding to CCSD(T)/6-31G(d) values the difference between the MP2/6-311G(d,p) and the MP2/6-31G(d) results. In addition, this extrapolation was shown earlier to give theoretical results in good agreement with the experimental ones for the neutral model system Me_2AlEt (see ref 18).

(d) Possible use of mixed basis set (6-311+G(2df,2pd) for the reactive part (e.g., olefin and chain) and 6-31+G(d,p) for the rest (e.g., metal and ligand)).

(e) Correction for longer polymer chains using hybrid DFT energy differences between the small (growing chain = ethyl) and the large (growing chain = butyl) system.

(f) BSSE corrections at the MP2 level. BSSE corrections to the olefin complexion energy are important in particular for post-HF calculations (MP2, CCSD(T)).[16] Obviously, this correction is not necessary if only the relative barriers for propagation and chain transfers (BHT or CHT) are needed.

Some of the important energy components of this model are reported in Table 7.

TABLE 7: Energy Components of the Multilayer Approach for the Ethylene Polymerization at Al (See Text for Details)[a]

	CC small system	MP2[b] Δ (basis)	DFT[c] Δ (system)	best extrapolation[d]	best DFT[e]	best value[f]
ΔE_{BHE}	12.3	1.9 (1.9)	−6.2	8.0 (8.0)	8.9	10.4
$\Delta E^{\#}_{\mathrm{BHE}}$	37.2	−0.7 (−1.8)	−5.6	30.9 (29.8)	28.4	31.0
ΔE_{coor}	17.6	−1.4 (−0.7)	−2.2	14.0 (14.7)	13.5	17.3
ΔE_{ins}	−7.5	−1.3 (−0.9)	0.0	−8.7 (−8.4)	−6.9	−7.5
$\Delta E^{\#}_{\mathrm{ins}}$	31.5	−2.2 (−3.3)	+0.4	29.7 (28.6)	28.7	28.9
$\Delta E^{\#}_{\mathrm{BHT}}$	25.4	−3.9 (−4.3)	−3.6	17.9 (17.5)	14.1	17.9

[a] In parentheses are reported the values for the MP2 extrapolation obtained with the largest basis set (6-311+G(2df,2pd)). [b] MP2 geometries, mixed basis set. [c] B1LYP, small basis set. [d] Obtained as sum of the values reported in the three previous columns. [e] B1LYP large basis set. [f] Best value = ΔE(CCSD(T)/6-31G(d)) + ΔE(MP2/6-31G(d)) − ΔE(MP2/6-311+G(2df,2pd)).

The resulting energies are in close agreement with our best estimates and are significantly better than those provided directly by the "best" DFT model (here B1LYP).

Although in this paper we focused our attention to the simple Al−amidinate system with $R^1 = R^2 = H$, it is worth nothing that analogous conclusions can be reached when bulky R^1 and R^2 amidinate substituents are considered, as well as for several other Al systems.[18]

4. Conclusion

In the present work, we have reported a detailed comparative study of DFT and post-HF approaches on ethylene insertion and chain transfer steps at a model cationic aluminum species. The size of the model and the high barriers involved make this system a suitable model for comparing the performances of different DFT models with refined post-HF methods.

The different nature of the reaction channels considered and the wide class of density functionals used (including classical GGA approximation, hybrid HF/DFT approaches and more recent τ-dependent functionals) allow us to obtain some significant computational insights from our calculations.

(1) The hybrid density functional methods always outperform classical GGA approaches, such as BP and BLYP. The poor results provided by these latter models prevent their systematic use for the study of catalytic reaction at aluminum centers. Concerning the other DFT models, we have found that the recent τ-dependent functionals are not yet as reliable as other DFT methods, giving nonsystematic errors in the energy evaluations.

(2) Among all the considered DFT approaches, the B1LYP hybrid functional provides the best performances with respect to the CCSD(T) results, although a significant discrepancy still remains for BHT termination. Because of an accidental compensation of chemical and computational models, the B1LYP energies for the ethyl system with a small basis set are close to those obtained at post-HF level for the large model with an extended basis set.

(3) Post-HF approaches show a significant basis set dependence for some of the reaction steps and in particular for those involving hydrogen transfer. Here the G3-like basis set does not provide converged results at the MP2 level and d functions on transferred hydrogen atoms are mandatory. In contrast, all DFT approaches give practically converged results at the 6-311G(d,p) level.

(4) The activation energy for the ethylene insertion is almost the same for a butyl chain or an ethyl chain at all levels of calculations. This confirms the validity of using an ethyl chain as a model to calculate the propagation step, at least in this particular case. The picture is different for the two chain termination mechanisms considered here. For the intermolecular β-hydrogen transfer to monomer, the use of a butyl chain lowers the activation energy by 3−4 kcal/mol at all levels of calculations; for the intramolecular β-hydrogen transfer to the metal, this lowering can reach 6 kcal/mol.

(5) Reliable energy estimates can be obtained by a mixed approach, in which geometries are obtained at the B1LYP level, single-point CCSD(T) energies are computed with a small basis set and the effects of basis set extension are evaluated at the MP2 are level, while the extension of the systems (i.e., the growing chain) is taken into account at the DFT level. This mixed approach seems to be valid for several neutral and cationic Al systems and might well be general. Our results also indicate how one can reduce the size of the basis set selectively for larger ligands.

On the basis of the above remarks, work is in progress in order to investigate the presence of similar effects (functional, basis set and chemical model) in other catalytic reactions, involving different metal centers.

Acknowledgment. The authors thank the CASPUR for computational time and technical assistance, the Italian and French Research Councils (CNR and CNRS) and Gaussian Inc. for financial support

Supporting Information Available: Details of the DFT energies (Table S-I) and of the MP2 computations using mixed basis sets (Table S-II); histogram representations of the activation energy for the hydrogen transfer to the chain (CHT) reaction (Figure S1) and for the β-hydrogen elimination reaction using a butyl chain (BHE_{bu}) (Figure S2). This material is available free of charge via the Internet at http://pubs.acs.org.

References and Notes

(1) Brintzinger, H. H.; Fisher, D.; Mülhaupt, R.; Rieger, B.; Waymouth, R. M. *Angew. Chem., Int. Ed. Engl.* **1995**, *34*, 1143.

(2) Britovsek, G. J. P.; Gibson, V. C.; Wass, D. F. *Angew. Chem., Int. Ed. Engl.* **1999**, *38*, 429.

(3) (a) Zhou, J.; Lancaster, S. J.; Walker, D. A.; Beck, S.; Thornton-Pett, M.; Bochmann, M. *J. Am. Chem. Soc.* **2001**, *123*, 223. (b) Chen, E. Y. X.; Marks, T. J. *Chem. Rev.* **2000**, *100*, 1391 and references therein.

(4) (a) Chan, M. S. W.; Ziegler, T. *Organometallics* **2000**, *19*, 5182 and references therein. (b) Lanza, G.; Fragalà, I. L.; Marks, T. J. *J. Am. Chem. Soc.* **2000**, *122*, 12764 and references therein.

(5) Kock, W.; Holthausen, M. C. *A Chemist's Guide to Density Functional Theory*; Wiley-VCH: Weinheim, Germany, 2000.

(6) Niu, S.; Hall, M. B. *Chem. Rev.* **2000**, *100*, 353.

(7) Adamo, C.; di Matteo, A.; Barone, V. *Adv. Quantum Chem.* **1999**, *36*, 4.

(8) van Voorhis, T.; Scuseria, G. E. *J. Chem. Phys.* **1998**, *109*, 400.

(9) Schmider, H. L.; Becke, A. D. *J. Chem. Phys.* **1998**, *108*, 9624.

(10) Hamprecht, F. A.; Cohen, A. J.; Trozer, D. J.; Handy, N. C. *J. Chem. Phys.* **1998**, *109*, 6264.

(11) Adamo, C.; Barone, V. *Chem. Phys. Lett.* **1997**, *274*, 242.

(12) Adamo, C.; Barone, V. *J. Chem. Phys.* **1999**, *110*, 6158.

(13) Adamo, C.; Talarico, G.; Barone, V., *Theor. Chem. Acc.*, submitted.

(14) Coles, M. P.; Jordan, R. F. *J. Am. Chem. Soc.* **1997**, *119*, 8125.

(15) Coles, M. P.; Swenson, D. C.; Jordan, R. F.; Young, V. G., Jr. *Organometallics* **1997**, *16*, 5183.

(16) Talarico, G.; Budzelaar, P. H. M.; Gal, A. W. *J. Comput. Chem.* **2000**, *21*, 398.

(17) Talarico, G.; Budzelaar, P. H. M.; Barone, V.; Adamo, C. *Chem. Phys. Lett.* **2000**, *329*, 99.

(18) Talarico, G.; Budzelaar, P. H. M. *Organometallics* **2000**, *19*, 5691.

(19) Woo, T. K.; Margl, P. M.; Lorenz, J. C. W.; Blöchl, P. E.; Ziegler, *J. Am. Chem. Soc.* **1996**, *118*, 13021.

(20) Thorshaug, K.; Støvneng, J. A.; Rytter, E.; Ystenes, M. *Macromolecules* **1998**, *31*, 7149.

(21) Frisch, M. J.; Trucks, G. W.; Schlegel, H. B.; Scuseria, G. E.; Stratmann, R. E.; Burant, J. C.; Dapprich, S.; Millam, J. M.; Daniels, A. D.; Kudin, K. N.; Strain, M. C.; Farkas, O.; Tomasi, J.; Barone, V.; Cossi, M.; Cammi, R.; Mennucci, B.; Pomelli, C.; Adamo, C.; Clifford, S.; Ochterschi, J.; Cui, Q.; Gill, P. M. W.; Johnson, B. G.; Robb, M. A.; Cheeseman, J. R.; Keith, T.; Petersson, Morokuma, K.; Malick, D. K.; Rabuck, A. D.; G. A.; Montgomery, J. A.; Raghavachari, K.; Al-Laham, M. A.; Zakrewski, V. G.; Ortiz, J. V.; Foresman, J. B.; Cioslowski, J.; Stefanov, B. B.; Nanayakkara, A.; Liu, J.; Liashenklo, A.; Piskorz, P.; Komaromi, I.; Challacombe, M.; Peng, C. Y.; Ayala, P. Y.; Chen, W.; Wong, M. W.; Andres, J. L.; Replogle, E. S.; Gomperts, R.; Martin, R. L.; Fox, D. J.; Binkley, J. S.; DeFrees, D. J.; Baker, J.; Stewart, J. P.; Head-Gordon, M.; Gonzalez, C.; Pople. J. A. *Gaussian 99*, Revision B.5+; Gaussian Inc.: Pittsburgh, PA, 2000.

(22) Æ. Frisch, M. J. Frisch, *Gaussian 98 User's Reference*; Gaussian, Inc.: Pittsburgh, PA, 1998, and references therein.

(23) Becke, A. *J. Chem. Phys.* **1993**, *98*, 5648.

(24) Adamo, C.; Barone, V. *J. Chem. Phys.* **1998**, *108*, 664.

(25) Perdew, J. P.; Ernzerhof, M.; Burke, K. *Phys. Rev. Lett.* **1998**, *80*, 891.

(26) Becke, A. *J. Chem. Phys.* **1996**, *104*, 1040.

(27) McLean, A. D.; Chandler, G. S. *J. Chem. Phys.* **1980**, *72*, 5639.

(28) Boys, S. F.; Bernardi, F. *Mol. Phys.* **1970**, *19*, 553.

(29) Barone, V.; Adamo, C. *J. Phys. Chem.* **1996**, *100*, 2094.

(30) Bauschlicher, C. W.; Ricca, A.; Partridge, H.; Langhoff, S. R. In *Recent Advances in Density Functional Methods*, Part II; D. P. Chonf Ed.; World Scientific: Singapore, 1997.

(31) Pople, J. A.; Head-Gordon, M.; Fox, D. J.; Raghavachari, K.; Curtiss, L. A. *J. Chem. Phys.* **1989**, *90*, 5622.
(32) Curtiss, L. A.; Raghavachari, K.; Redfern, P. C.; Pople, J. A. *J. Chem. Phys.* **1997**, *106*, 1063.
(33) Curtiss, L. A.; Raghavachari, K.; Redfern, P. C.; Rassolov, V.; Pople, J. A. *J. Chem. Phys.* **1998**, *109*, 7764.
(34) Curtiss, L. A.; Redfern, P. C.; Raghavachari, K.; Pople, J. A. *J. Chem. Phys.* **2001**, *114*, 108.
(35) Barone, V.; Adamo, C. *J. Chem. Phys*. **1996**, *105*, 11007.
(36) Sadhukhan, S.; Munoz, D.; Adamo, C.; Scuseria, G. E. *Chem. Phys. Lett*. **1999**, *306*, 83.
(37) Willis, B. G.; Jensen, K. F. *J. Phys. Chem*. *A* **1998**, *102*, 2613.
(38) Barone, V.; Orlandini, L.; Adamo, C. *J. Phys. Chem*. **1994**, *98*, 13185.
(39) Fangstrom, F.; Lunell, S.; Kasai, P. H.; Eriksson, L. A. *J. Phys. Chem.* **1998**, *102*, 1005.
(40) Petitjean, L.; Pattou, D.; Ruiz-Lopez, M. F. *J. Phys. Chem*. *B* **1999**, *103*, 27.
(41) Lorenz, J. C. W.; Woo, T. K.; Ziegler, T. *J. Am. Chem. Soc*. **1995**, *117*, 12793.
(42) Vyboishchikov, S. F.; Musaev, D. G.; Froese, R. D. J.; Morokuma, K. *Organometallics* **2001**, *20*, 309.
(43) Bauschlicher, C. W.; Partridge, H. *J. Chem. Phys*. **1995**, *103*, 1788.
(44) Baboul, A. G.; Curtiss, L. A.; Redfrern, P. C.; Raghavachari, K. *J. Chem. Phys*. **1999**, *110*, 7650.
(45) Francl, M. M.; Petro, W. J.; Hehre, W. J.; Binkley, J. S.; Gordon, M. S.; DeFrees, D. J.; Pople, J. A. *J. Chem. Phys*. **1982**, *77*, 3654.